ISSN No:-2456-2165

An Overall Discussion Mach-5 Spacecraft and Flight Dynamics Working Mechanics

ISSN No:-2456-2165

An Overall Discussion Mach-5 Spacecraft And Flight Dynamics Working Mechanics

Tonoy Sharma Tonmoy
A dissertation submitted in partial satisfaction of the requirements for the
Bachelor's of Engineering in Aircraft design &
Engineering in the Graduate Division Of the
NANCHANG HANKONG UNIVERSITY
25th May, 2020

LONGSHENG CHEN
Associate Professor,
School of Aircraft Engineering,
Nanchang Hangkong University
Nanchang, Jiangxi, China.
Mobile: 15350002862

ISSN No:-2456-2165

BACHELOR DEGREE THESIS ORIGINALITY STATEMENT

I thus announce that the accommodation and substance of the paper are because of the autonomous research done under the direction of the coach. Notwithstanding the substance of the content, this paper does exclude any type of research that has been utilized in the legitimate sense. It does exclude any papers or accomplishments that I have utilized in different applications the individual and aggregate, which makes significant commitments to the investigation of this paper, has been plainly shown in the content. I am completely mindful of the legitimate outcomes of this announcement without anyone else. EGREE THESIS COPYRIGHT USE AUTHORIZATION The creator of this proposition is to comprehend the principles and guidelines of the college about the booking and the utilization of the degree theory. I approve the Nanchang Hangkong University can be the all or part of the substance into the database were looked and methods for protection and assemblage of this thesis was repeated by copying, zoom or sweep.

ISSN No:-2456-2165

AN OVERALL DISCUSSION MACH-5 (HYPERSONIC) SPACECRAFT AND FLIGHT DYNAMICS WORKING MECHANICS

Abstract:- **Theoretical With the ability of fast flying, an increasingly dependable and cost efficient approach to get to space is given by hypersonic flight vehicles. Controller configuration, as key innovation to make hypersonic flight achievable and efficient, has various difficulties originating from huge flight envelope with outrageous scope of activity conditions, solid collaborations between flexible airframe, the impetus framework and the basic elements. This paper briefly presents a few ordinarily considered hypersonic flight elements, for example, winged-cone model, truth model, bend fitted model, control situated model and reemergence movement. Taking into account different plans, for example, linear zing at the trim state, input-yield linearization, trademark displaying, and back-venturing, the ongoing exploration on hypersonic flight control is looked into and the correlation is introduced. Flight dynamic characteristics are crucial in aircraft design. Simulation tools evaluate the aircraft statically and dynamical stability and maneuverability usually are based on a previously computed tabular aerodynamic model.To show the difficulties for hypersonic flight control, some specific qualities of hypersonic flight are talked about and the potential future research is tended to with managing actuator elements, streamlined/response fly control, flexible effect, non-least stage issue and elements association. A new model is developed to more accurately capture the dynamics and control of an air-breathing hypersonic vehicle using a computationally inexpensive formulation. The vehicle model integrates a scramjet engine analysis tool developed specifically for use in a control-oriented model and a six-degree-of-freedom rigid-body flight dynamics model. The combined hypersonic vehicle model requires less than ten seconds with a single 2.6 GHz processor to calculate the total thrust, lift, and aerodynamic moment on the vehicle. The inlet and nozzle analysis handles shock-shock and shock-expansion interactions, and expansions are considered to be a series of discrete waves. The combustor model utilizes scaling laws that retain some of the fidelity of higher-order simulations. On the parts of the vehicle that are not part of the propulsive flowpath, modified shock-expansion theory is used to calculate the pressure. In this approach the role of the propulsive model will be only to calculate the net forces and moments on the inlet, combustor, and nozzle. The result is a control-oriented hypersonic vehicle model that qualitatively captures the nonlinear interactions between vehicle dynamics and the scramjet engine.**

Keywords:- *Hypersonic flight vehicle, linearizing at the trim state, input-yield linearization, back-venturing, non-least phase.*

ISSN No:-2456-2165

TABLE OF CONTENTS

ISSN No:-2456-2165

CHAPTER 1

INTRODUCTION

Among the many challenges facing the development of air-breathing hypersonic vehicles is maintaining controlled flight and an In addition to maximizing fuel efficiency, ensuring adequate thrust and lift, and limiting heat transfer, the vehicle has to be able to balance all of the forces on it. In order to balance these forces in a simulation, a model is required that can evaluate the performance of the entire vehicle in a few seconds or less. Additionally, flight at such high speeds causes complex interactions among the airframe, propulsions system, vehicle aerodynamics, and other aspects. As a result, it is not possible to design each component of the vehicle independently. Therefore a fast model that can analyze a range of vehicles can also be useful to assist the design of a hypersonic vehicle. The overall goal of this hypersonic vehicle modeling effort is to create a three-dimensional flight simulation framework that includes coupled inertial, aerodynamic, propulsive, elastic, and thermal analysis in such a way to enable accurate control simulation. The model should be accurate to within 10% and able to analyze a vehicle in a few seconds or less on a single-processor computer. In addition to high-fidelity hypersonic vehicle analysis by Candler et al., 1,2 Higgins and Schmidt and many others, there has been a considerable effort to develop low-order hypersonic vehicle simulations that can run in short time periods using only moderate computational resources. Oppenheimer et al.4, 5 and Chavez and Schmidt6 have developed longitudinal (two-dimensional) hypersonic flight dynamics [2] models that can be used to simulate a variety of vehicle trajectories. Mirmirani et al.8 investigated merging experimental and computational data to generate control algorithms for hypersonic vehicles. At the same time, progress has been made by O'Brien et al.8 and Torrez et al.9, 10 in developing fast simulations of air-breathing hypersonic propulsion systems. The present work aims to extend a three-dimensional flight dynamics model11 by including a more accurate propulsion model. Our approach is to separate the vehicle into portions that are part of the propulsive system and portions that are not. We model the propulsive components, i.e., the inlet, 12 combs, 10 and nozzle, 13 using a two-dimensional representation that has the required fidelity for propulsive analysis. We analyze the remaining portions of the vehicle using a simpler three-dimensional model that only calculates the pressure and temperature on the vehicle surfaces. The use of a two-dimensional model [5] for some parts of the vehicle limits the types of geometries that the proposed model can analyze. For example, the approach cannot be used for a vehicle with an inward-turning inlet2 or a conical- type nozzle. However, for hypersonic vehicles similar to those shown in Fig. 1, the proposed approach should be relatively accurate because the portions that are modeled as two-dimensional do not vary much in throne of the directions normal to the free stream flow. In this paper all analysis is of the geometry provided by VSI Aerospace, some of the parts from An important contribution of this work is the development of a nonlinear adaptive controller for the 6-DOF control design model. The controller was endowed with a modular structure, comprised of an adaptive inner-loop attitude controller and robust nonlinear outer-loop controller of fixed structure. The purpose of the outer-loop controller is to avoid the typical complexity of solutions derived from adaptive backstopping methods. A noticeable feature of the outer-loop controller is the presence of an internal model unit that generates the reference for the angle-of-attack, in spite of parametric model uncertainty. Airspeed, lateral velocity, vehicle's heading and altitude were considered as regulated outputs of the system. Simulation result son the control simulation model show the electiveness of the developed controller inspire of significant variation in the flight parameters.

ISSN No:-2456-2165

A. Hypersonic

Through decades of aircraft and spacecraft design, traveling at ever increasing speeds has always been a long-running objective. Within the realm of supersonic air-breathing vehicles, there has been the Concorde, a supersonic transport vehicle and the SR-71, a supersonic stealth reconnaissance aircraft. Beyond supersonic speeds, there is the subsequent flight regime of hypersonic speeds which is generally classified as traveling at speeds greater than Mach 5. The first vehicle to achieve hypersonic flight was a WAC Corporal boosted by a German V-2 rocket, which reached maximum velocity of just over 5000 mph. In the decades to follow, numerous hypersonic vehicles have emerged such as the X-43, X-51, Apollo mission capsules, and space shuttles. For the space shuttle and Apollo capsules, re-entry velocities reached Mach 25 all the way to Mach 36. As design and analysis tools have progressed, hypersonic research and development have been revitalized. The surge is fueled in large part due to foreign powers, such as China and Russia, developing and testing hypersonic technologies. According to the Business Insider, the US Air Force has already awarded contracts to develop these new capabilities. While foreign powers have tested capabilities, it is suspected that the hypersonic vehicles will not be deployed for another 3-5 years. The vehicles are of great concern because they travel at such high speeds that it becomes difficult to track and intercept. Previously, hypersonic technology development has been hindered due to fluctuations in investment and deficiencies in computational tools to perform the necessary analyses. Now with near billion-dollar development contracts being awarded by the government, companies and academia cannot afford to be wasteful with the massive amount of funding that is being directed towards hypersonic. The development of hypersonic vehicles can directly impact defense capabilities, transport times, and less expensive method to access space. In the subsonic regime, it is safe to assume that the density of the air is constant when the free stream Mach number is less than or equal to 0.3. Beyond Mach 0.3, flows are considered to be compressible. In the supersonic and hypersonic regime, the flow around an object is characterized by the shock waves that form. Shock waves are pressure waves generated from a body traveling at supersonic speeds. Hypersonic air vehicles are sensitive to changes in flight condition as well as physical and aerodynamic parameters due to their design and flight conditions of high altitudes and Mach numbers. For example, at cruise flight at altitude of 110,000 ft and Mach 15, a 1-deg increase in angle of attack produces a load factor of about 0.33 g. Furthermore, it is difficult to measure or estimate the atmospheric properties and aerodynamic characteristics at the hypersonic flight altitude. As a result, modeling inaccuracies can result and can have strong adverse effects on the performance of air vehicle's control systems. The pressure waves coalesce, forming a large compression wave at the front of a body. An essential aspect of hypersonic flow is the strength of shock waves which causes the boundary layer also grows to be very large around the vehicle surface. In addition, across the shock wave, thin shock layers forms where flow properties change drastically; pressure, density, and temperature increase behind the shock wave while the Mach number decreases. These changes in the flow properties directly affect the lift, drag, pressure, aerodynamic heating, and controllability of the vehicle. The change in various properties shows that the disciplines involved in designing a hypersonic vehicle are highly coupled.

B. Hypersonic flight dynamics

In literature, there have been several papers discussing the modeling of hypersonic flight dynamics. In the winged-cone accelerator configuration and the X-30 one are analyzed in de- tail as such it will not be discussed in detail here. The readers could refer to [7,2,3] for more details. However, to show how the control approaches in Section 3 are developed, several kinds of the widely studied nonlinear hypersonicflight dynamics with aerodynamic pram are presented in this section. We can find out this answer that what is flight dynamics? .Flight dynamics is the science of air vehicle orientation and control in three dimensions. The three critical flight dynamics parameters are the angles of rotation in three dimensions about the vehicle's center of gravity (cg), known as pitch, roll and yaw. Control systems adjust the orientation of a vehicle about its cg. A control system includes control surfaces which, when deflected, generate a moment (or couple from ailerons) about the cg which rotates the aircraft in pitch, roll, and yaw. For example, a pitching moment comes from a force applied at a distance forward or aft of the cg, causing the aircraft to pitch up or down. Roll, pitch and yaw refer to rotations about the respective axes starting from

ISSN No:-2456-2165

a defined steady flight equilibrium state. The equilibrium roll angle is known as wings level or zero bank angle. The most common aeronautical convention defines roll as acting about the longitudinal axis, positive with the starboard (right) wing down. Yaw is about the vertical body axis, positive with the nose to starboard. Pitch is about an axis perpendicular to the longitudinal plane of symmetry, positive nose up.[1]A fixed-wing aircraft increases or decreases the lift generated by the wings when it pitches nose up or down by increasing or decreasing the angle of attack (AOA). The roll angle is also known as bank angle on a fixed-wing aircraft, which usually "banks" to change the horizontal direction of flight. An aircraft is streamlined from nose to tail to reduce drag making it advantageous to keep the sideslip angle near zero, though an aircraft may be deliberately "side slipped" to increase drag and descent rate duringlanding, to keep aircraft heading same as runway heading during cross-wind landings and during flight with asymmetric power.

Fig. 1: Hypersonic vehicle

C. Importance of hypersonic vehicles

Hypersonic vehicles are perhaps a dream of the future, but if they have chance of happening, research is important to develop materials that will handle the high temperatures created at hypersonic speeds. Anything travelling faster than Mach 5 is hypersonic. Developing a hypersonic scramjet vehicle; there is a group of researchers trying to develop air-breathing hypersonic vehicles that will work at low altitudes for sustained periods of time. These air-breathing engines are called scramjets (supersonic combustion ramjet).Air is forced into a reaction chamber and then reacts with the fuel. The combusted material is propelled out the back end to make the vehicle experience a reaction force, which pushes it forwards. A scramjet vehicle is much lighter than an equivalent rocket because it doesn't need to carry a supply of oxygen to react with the fuel. In 2010, another experimental vehicle called the X-51 Wave rider had a scramjet burn time of 140 seconds and reached a speed of Mach 5.If scramjet technology can be developed to produce a vehicle that can fly for extended periods of time, it may be possible to fly to the other side of the world in 2 hours! There are many challenges that need to be met before this could ever become a reality.Why a new protective material is needed; one of the challenges to be solved is to develop a material that will handle the 2000 °C temperatures that would be generated at those speeds. These temperatures are created because the vehicle is slamming into the air particles faster than the particles can get out of the way. Current hypersonic experimental vehicles are only able to travel at these speeds for a short time before the material on the outside breaks down. Metal would not be suitable for a hypersonic vehicle because the melting point is lower than the 2000°C that would be encountered. For example, titanium was used for the supersonic SR-71 Blackbird, but it has a melting point of 1668°C. The vehicle material also needs to be able to resist violent chemical attacks. At the high temperatures and pressures encountered, oxygen will break apart the molecular bonds of any structure that is not strong enough to handle it. Ablation, insulation and active cooling; There are several ways of protecting space vehicles from extreme temperatures. Even if a new heat-protective material could be developed, other technologies would still be needed to keep a hypersonic vehicle from overheating ablative materials – a sacrificial layer is placed on the outside of the structure. As it heats up, tiny bits of the ablative material break away and carry the heat energy with it. Ablative materials are not reusable. Insulation – thick ceramic tiles were placed over the Space Shuttle orbiter (SSO) to stop the heat

ISSN No:-2456-2165

from reaching the inside. Thick tiles will not be suitable for a hypersonic vehicle because of a need for lightens. Active cooling – for a liquid fuel engine; the cold fuel can be pumped through pipes near the hottest parts of the rocket engines before it is pumped into the reaction chamber. A different method is to use heat pipes near the surface on the front edge of a vehicle. These pipes use evaporation and condensation cycles inside the pipes to transfer the heat away from the hottest part.

ISSN No:-2456-2165

CHAPTER 2

GEOMETRY OF HYPERSONIC VEHICLES

Traditional MPC show that tube-MPC is more effective, and it has lower computation complexity and strong practicability. The rest of this article is organized as follow. In “Vehicle model” section 2, the nonlinear model of hyper- sonic vehicle is presented. The polytypic LPV modeling is given in “Polytypic LPV model” section. A tube-MPC con- droller is designed in “Design of the tube-MPC controller” section. In “Simulations” section, simulations are given. Finally, we conclude this article in the last section. Given that the below;

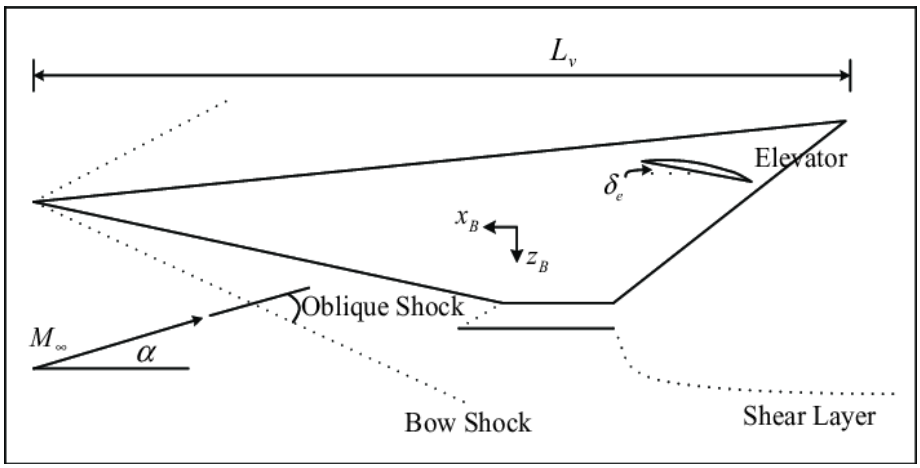

Fig. 2: Geometry of hypersonic vehicle model

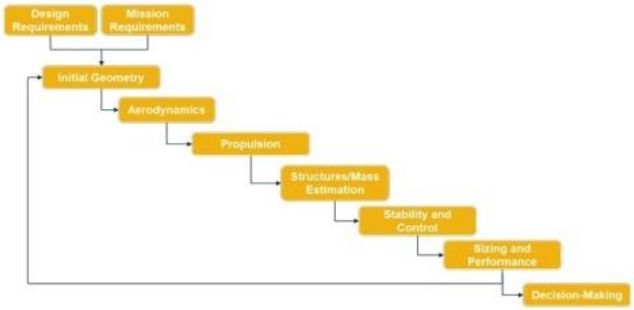

Fig. 3: Sequal design

Fig. 4: Hypersonic design discipline coupling

ISSN No:-2456-2165

A. Hypersonic vehicles characteristics

In aerodynamics, a hypersonic speed is one that greatly exceeds the speed of sound, often stated as starting at speeds of Mach 5 and above. The precise Mach number at which a craft can be said to be flying at hypersonic speed varies, since individual physical changes in the airflow (like molecular dissociation and ionization) occur at different speeds; these effects collectively become important around Mach 5-10.The hypersonic regime can also be alternatively defined as speeds where specific heat capacity changes with the temperature of the flow as kinetic energy of the moving object is converted into heat. Characteristics of flow: While the definition of hypersonic flow can be quite vague and is generally debatable (especially due to the absence of discontinuity between supersonic and hypersonic flows), a hypersonic flow may be characterized by certain physical phenomena that can no longer be analytically discounted as in supersonic flow [13]. The peculiarity in hypersonic flows is as follows: 1. Shock layer,2. Aerodynamic heating,3. Entropy layer 4. Entropy layer,5. Low density effects, 6. Independence of aerodynamic coefficients with Mach number.

As a body's Mach number increases, the density behind a bow shock generated by the body also increases, which corresponds to a decrease in volume behind the shock due to conservation of mass. Consequently, the distance between the bow shock and the body decreases at higher Mach numbers. As Mach numbers increase, the entropy change across the shock also increases, which results in a strong entropy gradient and highly vertical flow that mixes with the boundary layer. Entropy layer; As Mach numbers increase, the entropy change across the shock also increases, which results in a strong entropy gradient and highly vertical flow that mixes with the boundary layer. Viscous interaction: A portion of the large kinetic energy associated with flow at high Mach numbers transforms into internal energy in the fluid due to viscous effects. The increase in internal energy is realized as an increase in temperature. Since the pressure gradient normal to the flow within a boundary layer is approximately zero for low to moderate hypersonic Mach numbers, the increase of temperature through the boundary layer coincides with a decrease in density. This causes the bottom of the boundary layer to expand, so that the boundary layer over the body grows thicker and can often merge with the shock wave near the body leading edge. High temperatures due to a manifestation of viscous dissipation cause non-equilibrium chemical flow properties such as vibrational excitation and dissociation and ionization of molecules resulting in convective and radiative heat-flux. The categorization of airflow relies on a number of similarity parameters, which allow the simplification of a nearly infinite number of test cases into groups of similarity. For transonic and compressible flow, the Mach and Reynolds numbers alone allow good categorization of many flow cases. Hypersonic flows, however, require other similarity parameters. First, the analytic equations for the oblique shock angle become nearly independent of Mach number at high (~>10) Mach numbers. Second, the formation of strong shocks around aerodynamic bodies means that the free stream Reynolds number is less useful as an estimate of the behavior of the boundary layer over a body (although it is still important). Finally, the increased temperature of hypersonic flows means that real gas effects become important. For this reason, research in hypersonic is often referred to as (Chaofang Hu1, 2007)aerothermodynamics, rather than aerodynamics. The introduction of real gas effects means that more variables are required to describe the full state of a gas. Whereas a stationary gas can be described by three variables (pressure, temperature, adiabatic index), and a moving gas by four (flow velocity), a hot gas in chemical equilibrium also requires state equations for the chemical components of the gas, and a gas in non-equilibrium solves those state equations using time as an extra variable. This means that for a non-equilibrium flow, something between 10 and 100 variables may be required to describe the state of the gas at any given time. Additionally, rarefied hypersonic flows (usually defined as those with a Knudsen number above 0.1) do not follow the Navier–Stokes equations. Hypersonic flows are typically categorized by their total energy, expressed as total enthalpy (MJ/kg), total pressure (kPa-MPa), stagnation pressure (kPa-MPa), stagnation temperature (K), or flow velocity (km/s). Wallace D. Hayes developed a similarity parameter, similar to the Whitcomb area rule, which allowed similar configurations to be compared. Hypersonic flow can be approximately separated into a number of regimes. The selection of these regimes is rough, due to the blurring of the boundaries where a particular effect can be found.

ISSN No:-2456-2165

B. Modeling method for hypersonic vehicle

The focus of this paper is to integrate a three-dimensional, six-degree-of-freedom flight dynamics model, a first principle model of the 6-DOF dynamics of a generic hypersonic vehicle, an un- steady aerodynamic model, and a control-oriented model. [35] The flight dynamics model consists of the six-degree-of-freedom rigid body equations of motion coupled with a simple unsteady aerodynamic model. The aero- dynamic model, determines the aerodynamic forces and moments acting over the vehicle. However, because the inlet, isolator, combustor, and nozzle are so tightly coupled, the propulsion model is responsible for analyzing the inlet and nozzle in addition to the isolator and combustor. In our proposed model, the vehicle itself consists of many polygonal surfaces. Each of these polygons is either a part of the propulsive system, part of the remaining vehicle, or on the border between the two. The results of both components are combined to generate a net force and moment on the vehicle, which can be used in a rigid-body flight dynamics simulation. This is an improvement over previous formulations because it combines a fast, higher-fidelity model of the propulsion system with a model of a complete hypersonic vehicle in a six-degree-of-freedom simulation framework.

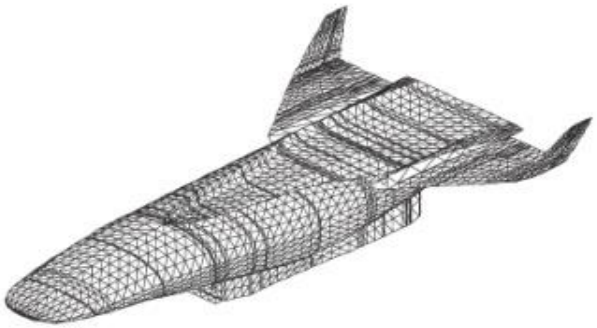

Fig. 5: Isometric view of hypersonic vehicle used in this analysis

The six-degree-of-freedom rigid body equations of motion are derived using a Newtonian approach, assuming a flat- earth inertial reference frame. The translational velocity vector, ~vB, and rotational velocity vector, ω~B, are expressed in a body-fixed reference frame whose origin is located at an arbitrary fixed point on the vehicle. During long-duration simulation of free flight, a hypersonic vehicle is expected to consume a significant portion of its total mass in fuel. Therefore the rigid body equations of motion are written for a vehicle with varying inertial properties (total mass, center of mass location, etc.). These equations of motion take the form

$$\begin{bmatrix} m & -m\tilde{r}_{CM} \\ m\tilde{r}_{CM} & I_B \end{bmatrix} \begin{Bmatrix} \dot{\vec{v}}_B \\ \dot{\vec{\omega}}_B \end{Bmatrix} + \begin{bmatrix} m\tilde{\omega}_B & -m\tilde{\omega}_B\tilde{r}_{CM} \\ m\tilde{r}_{CM}\tilde{\omega}_B & \tilde{\omega}_B I_B \end{bmatrix} \begin{Bmatrix} \vec{v}_B \\ \vec{\omega}_B \end{Bmatrix} = \begin{Bmatrix} \vec{F}_B \\ \vec{N}_B \end{Bmatrix}$$

where m is the vehicle mass, rCM is the position of the center of mass with respect to the body-fixed reference frame, ˜(·) is the skew-symmetric matrix operator, and IB is the inertia matrix with respect to the center of mass. The external forces, ~ FB, and moments, ~ MB, come the vehicle aerodynamics, propulsion system, and gravity. The aircraft attitude is expressed using the roll (φ), pitch (θ), and yaw (ψ) Euler angles. The Euler angle kinematics are related to the rigid body rotational velocity by

$$\begin{Bmatrix} \dot{\phi} \\ \dot{\theta} \\ \dot{\psi} \end{Bmatrix} = \begin{bmatrix} 1 & \sin(\phi)\tan(\theta) & \cos(\phi)\tan(\theta) \\ 0 & \cos(\phi) & -\sin(\phi) \\ 0 & \frac{\sin(\phi)}{\cos(\theta)} & \frac{\cos(\phi)}{\cos(\theta)} \end{bmatrix} \begin{Bmatrix} \omega_{B,x} \\ \omega_{B,y} \\ \omega_{B,z} \end{Bmatrix}$$

The position of the vehicle is expressed in terms of the earth-fixed inertial reference frame. The inertial position kinematics are related to the Euler angles and rigid body translational velocity through.

$$\begin{Bmatrix} \dot{x}_E \\ \dot{y}_E \\ \dot{z}_E \end{Bmatrix} = R_{EB}(\phi, \theta, \psi) \begin{Bmatrix} v_{B,x} \\ v_{B,y} \\ v_{B,z} \end{Bmatrix}$$

a) Aerodynamics model

We have developed a simple medication to two-dimensional shock-expansion theory to develop a model that is relatively accurate in all regions and based on well-established compressible flow physics with Minomodification. This method is a local inclination method, i.e., the pressure at any point on the surface of the vehicle is determined by that point's total velocity and orientation (and independent of the geometry of the rest of the vehicle). [24] For each surface, as shown in Fig. 1, a local pressure is calculated, which is multiplied by the area of the triangle to determine the force applied on each surface. Then the incident velocity on the surface is

$\vec{v} = \vec{v}_\infty + \vec{\omega} \times \vec{r}$

Where $\vec{v}_\infty$ is the freestream (vehicle) velocity, $\vec{\omega}$ is the angular velocity of the vehicle, and $\vec{r}$ is the vector from the vehicle's center of mass to the center of the current surface. The deflection angle δ is given by

$$\sin \delta = - \frac{\check{n}.\vec{v}}{\| v \|}$$

Where $\check{n}$ is the unit normal to the surface. We then convert the incident velocity into a Mach number using $M = \| v \| \sqrt{\frac{\rho_\infty}{\gamma \rho_\infty}}$, Where γ is specific heat ratio. If δ < 0, Prandtl-Meyer t Otherwise the pressure is calculated using the formula

$$P = P_\infty \left(\frac{2\gamma}{\gamma+1} M^2 \sin^2 \beta - \frac{\gamma+1}{\gamma-1} \right)$$

If the defection angle is sufficiently small, it is possible for an attached shock wave to exist, and the shock angle calculated using the implicit formula

$$\tan \delta = 2 \cot \beta \frac{M^2 \sin 2\beta - 1}{M^2 (\gamma + \cos 2\beta) + 2}$$

The maximum value for the shock angle is

$$\sin^2 \beta_{max} = \frac{(\gamma+1)M^2 - 4 + \sqrt{(\gamma+1)^2 M^4 + 8(\gamma^2 - 1)M^2}}{4M^2\gamma}$$

ISSN No:-2456-2165

Which leads to a maximum defection angle by substituting the result of (9) into (8)If the defection angle is too large for an attached shock, i.e., $\delta > \delta max$, the wave angle is given by an interpolation;

$$\beta = \beta_{max} + \frac{\delta - \delta_{max}}{\pi/2 - \gamma_{max}} + (\pi/2 - \beta_{max})$$

This aerodynamic model corresponds to a normal shock if the defection angle is exactly 90◦. In light of this, our model avoids large errors for all possible inclination angles.

The propulsion model can further be split into three components: the inlet, the combustor, and the nozzle. In the scramjet mode, neither component affects the one upstream of it, and the three parts can be solved in sequence. In ramjet mode the flow through the combustor section is subsonic, and signals can travel upstream, but we are only considering scramjet-mode operation in the present analysis. This also means that the isolator, which is the portion of the engine towpath between the inlet and the combustor section, can be largely ignored.

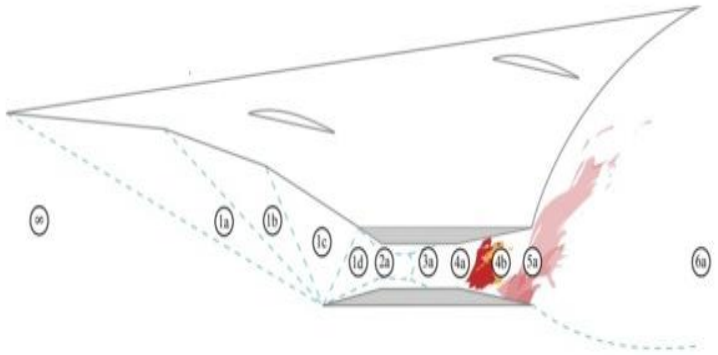

Fig. 6: an example of geometry. The station numbers are extensible by adding successive letters to each station for a more complex geometry

The inlet model considers scramjet inlet designs that are approximately two-dimensional. A satisfactory control- oriented model must require a relatively small amount of computational time and still yield a relatively accurate solution for the inlet flow. Instead of solving directly for the flow conditions at each point in the flow, as is done in computational fluid dynamics (CFD), our method solves for the positions of the relevant waves, which separate regions in which the flow properties are considered to be uniform. The locations of the shock waves and expansions are determined using established two-dimensional supersonic theory.. To make this possible in a digital computing environment, expansion fans are approximated as a number of discrete isentropic waves. In many ways this is a generalized and automated version of the method of characteristics. This method has been described in several previous papers.

The output of this inlet model is a set of polygons, each with an associated set of thermodynamic conditions (density, pressure, temperature, Mach number, and flow direction). The result resembles the output of two-dimensional CFD, as shown in the comparison in Fig. 3. The reduced-order solution and CFD solutions are shown for the same inlet flying at a flight Mach number of $M\infty = 10.0$ and angle of attack of $\alpha = 0$.

ISSN No:-2456-2165

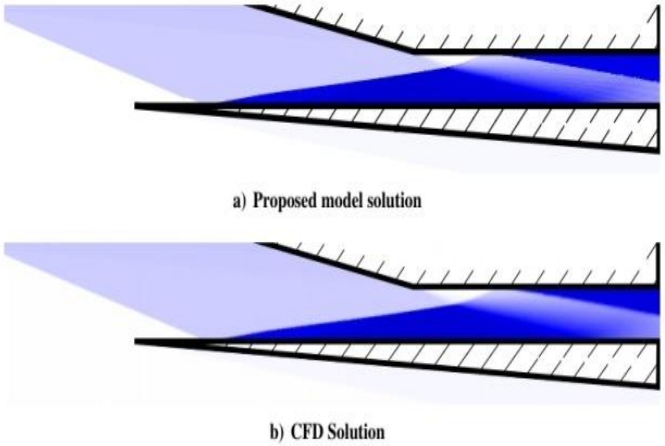

Fig. 7: Proposed model and CFD Solution

Darker shades of blue represent regions of higher pressure; white represents free stream pressure and black represents p/p∞ = 90.For critical importance to the inlet model is the discretization of expansion fans. An expansion fan can be seen in both graphics of Figure starting at the corner in the upper surface. Prandtl-Meyer theory can be used to obtain the exact solution to this type of flow. However, this result is continuous, and needs to be modeled as a discrete change in some way to be useful in our model. Unfortunately, any attempt to discredited the Prandtl-Meyer expansion results in a approximation that does not conserve momentum.13 Our approach is to model the expansion as a series of weak expansion shocks, which is a close approximation to Prandtl-Meyer theory and conserves mass, momentum, and energy. The geometry and an example of a discredited expansion are shown in Fig. 4. Another critical modeling problem occurs when two waves intersect each other. The inlet model resolves this situation by solving a two-dimensional Riemann problem.10 finally, the combustor model assumes that the flow leaving from the inlet is uniform (i.e., does not vary with coordinates normal to the flow direction). To match this constraint with the two-dimensional result from the inlet analysis, we select the thermodynamic state in the combustor so that the total fluxes of mass, momentum, and energy are equal at the end of the inlet and the beginning of the combustor.

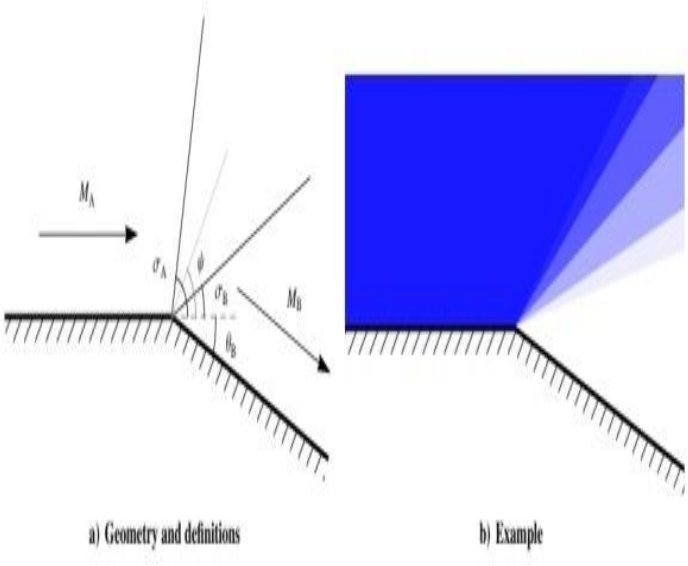

Fig. 8: Geometry shown darker shades of blue represent higher pressures

ISSN No:-2456-2165

b) Nozzle

To accurately predict thrust, a nozzle model must analyze the expansion and acceleration of the exhaust gases from the combustor. In a typical scramjet nozzle, the lower edge of the exhaust plume is a slip stream, and its location varies according to combustor and flight conditions.

An example of a scramjet nozzle. The temperature in the combustor section reaches temperatures high enough to cause significant dissociation of the gas, which means that at the beginning of the nozzle, some of the combustion products will be split into smaller molecules. However, the temperature drops dramatically in the nozzle, and these smaller molecules, e.g., N and O, will recombine into stable molecules such as N2 and O2. In most flows, the release of energy caused by such a chemical change would have a significant effect. However, the velocities are so large in scramjet nozzles that the chemical energy release is small compared to the kinetic energy of the flow [13] for that reason, and because it would slow down the computation, we do not consider chemistry in the nozzle. In addition, it is crucial to determine the streamline that forms the lower edge of the exhaust plume. This stream- line determines the effective area of the nozzle and thus is has a significant effect on the total thrust of the nozzle. Calculating this streamline using a one-dimensional model would be impossible because information in a supersonic flow travels along characteristics, which are the lines shown in Fig. 4. Previous models have considered one-dimensional models with several simplifying assumptions 5,6,16 .Because the nozzle does not have the sensitive behavior of the inlet, these one-dimensional models can produce a representative approximation of the forces on the nozzle. However, even if it were possible to determine the location of the exhaust plume, a one-dimensional model gives inaccurate thrust predictions.[13]We solve this problem by modeling the nozzle using a slight.

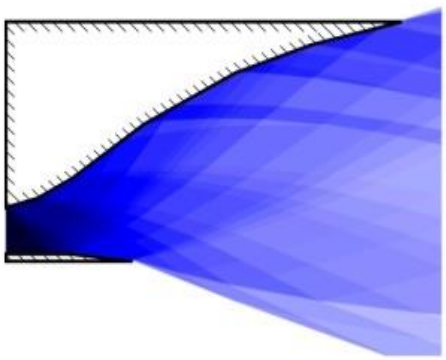

Fig. 9: Reduced-order solution of example scramjet nozzle

The combustion code marches the flow conservation equations from the beginning of the combustor to the end of the internal nozzle all flow states are allowed to vary in the downstream axial direction. To keep the model one-dimensional, only derivatives with respect to the axial coordinate are considered. Some quantities, such as jet spreading and mixing, vary in the transverse directions, but they may only vary algebraically such that their evolutions do not depend on the information propagating downstream. The conservation equations, along with the equation of state, form the basis of the model. By taking derivatives in the x-direction, these give a set of ordinary differential equations. The simultaneous solution provides all the information needed to calculate the evolutions of the state variables (p, ρ, T) and the heat release through the duct. The two simplest differential equations used in the propulsion model follow. In these equations, W is the average molecular weight of the gas, and A is the area of the combustor duct as a function of x. The equation of state takes the form

$$\frac{1}{p}\frac{dp}{dx} = \frac{1}{T}\frac{dT}{dx} + \frac{1}{\rho}\frac{d\rho}{dx} - \frac{1}{W}\frac{dW}{dx}$$

ISSN No:-2456-2165

Which comes from differentiating the equation of state, p = ρRT. The conservation of mass gives

$$\frac{1}{\rho}\frac{d\rho}{dx} = \frac{1}{\dot{m}}\frac{d\dot{m}}{dx} - \frac{1}{u}\frac{du}{dx} - \frac{1}{A}\frac{dA}{dx}$$

Where $\dot{m}$ is the mass flow rate through the duct, and d $\dot{m}$/dx represents the mass flow rate of fuel added as a function of x. The total mass flow rate of fuel added is

$$\dot{m}_f = \int \frac{d\dot{m}}{dx}\, dx$$

The fuel-air equivalence ratio, Φ, is the ratio of the fuel mass flow rate to the maximum amount of fuel that could burn based on the amount of oxygen in the combustor. The conservation of momentum states

$$\frac{1}{u}\frac{du}{dx} = -\frac{1}{\rho u^2}\frac{dp}{dx} - \frac{1}{\dot{m}}\frac{d\dot{m}}{dx}$$

If we define a mass-averaged specific heat as

$$\bar{c}_p = \sum_{i=1}^{n_{sp}} c_{p,i} Y_i$$

And neglect viscous forces, the conservation of energy take the form

$$\frac{\bar{c}_p}{h_0}\frac{dT}{dx} = \sum_{i=1}^{n_{sp}} \left(\frac{1}{\dot{m}}\frac{d\dot{m}_i}{dx} - \frac{dY_i}{dx} \right) \frac{h_i}{h_0} - \frac{u}{h_0}\frac{du}{dx} - \frac{1}{\dot{m}}\frac{d\dot{m}}{dx}$$

These are essentially the equations used in the combustor model. The rates of change for each species, dY_i/dx, are calculated at each point in the combustor using a amulet model. For design there are two largely disparate models in our proposed method of analysis for the hypersonic vehicle. In particular the models used in conjunction with the propulsion model are two-dimensional, and the models used with the aerodynamic model are three-dimensional. Since the aerodynamic model does not accurately compute the conditions in the gas away from the surface of the vehicle, it cannot be used to accurately model the propulsion. Likewise, the propulsion model cannot predict the three-dimensional forces necessary for a six-degree-of-freedom simulation. Thus we are forced to use both models, and we must determine for each of the vehicle's surfaces which model to use. In addition, we must extract the two-dimensional geometries to use with the propulsion model. We have developed an automated utility to complete both of these tasks, and the result is visualized in this figure. The surfaces in red are part of the inlet or nozzle, and the boundary between these regions and the rest of the vehicle is shown with a thick black line. The traces of the two-dimensional geometries used in the propulsive model are shown.

ISSN No:-2456-2165

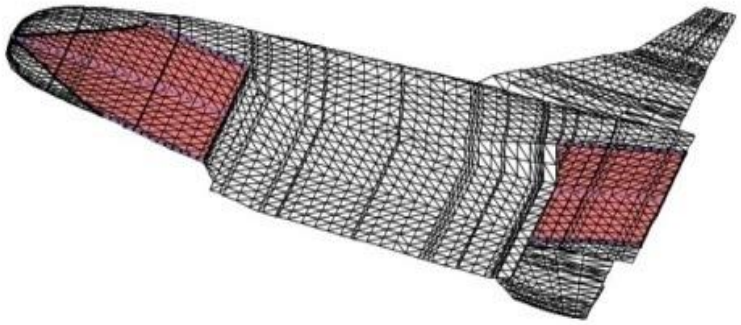

Fig. 10: Lower side of hypersonic vehicle with cells in the propulsive flow path shown as red and the two-dimensional cuts shown with the blue dashed line.

c) Region determination

Figuring out which surfaces are a piece of the isolator and combustor is moderately simple since they are the surfaces encircled by the cowl. The vast majority of the work is in deciding the geometry of the channel and spout. Our general way to deal with this is to begin with focuses on the edge of the gulf cowl or spout cowl and follow smoothes out in the fitting headings. For example, to follow the limit of the gulf, we start with the three focuses: the left, focus, and right purposes of the channel cowl. In this fig; these are the two right-most corners of the bay pentagon and the point in the edge joining those two corners. Beginning with those three focuses, we follow the crossing point of the vehicle and a plane containing that point and unit vectors pointing in the flow course and vertical heading. This equivalent procedure is rehashed for the other two gulf cowl focuses, which creates the three blue dabbed lines in the delta locale of Figure. At long last, lines are followed along the surface to join the endpoints of the three blue spotted lines. At that point the whole procedure is rehashed for the spout.

d) Engine Flow path

To restrain the unfriendly impacts of utilizing a two-dimensional model on certain pieces of the vehicle, the impetus code is run twice for every reproduction of the vehicle. This is the reason for the three spotted lines in Fig. Note that solitary two computations are vital on the grounds that the left and right flow ways are indistinguishable from one another.

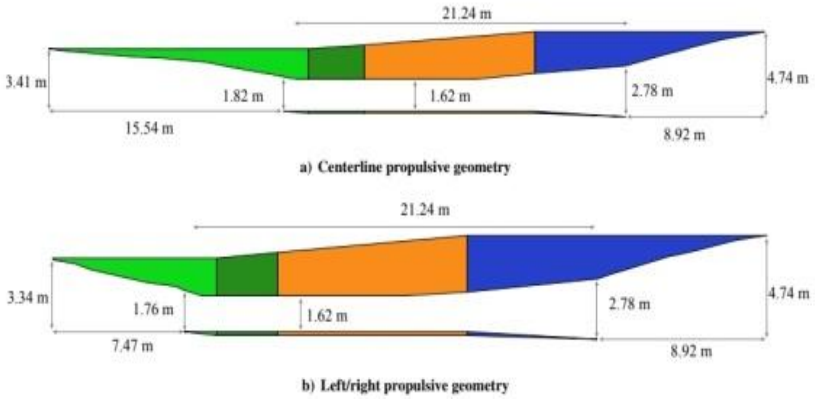

Fig. 11: Schematics of two-dimensional propulsive flow path geometries

ISSN No:-2456-2165

The output of the propulsive calculations is a force per unit width and moment per unit width at the nose of each two-dimensional section. Since the propulsive geometry is two-dimensional, it is not possible to calculate a force and moment directly. If ~ F0CL is the force per unit width of the centerline flow path and ~ F0 L is the force per unit width of the other flow path geometry, the total force from the propulsion system is

$$\vec{F} = (\mathcal{Y}CL - \mathcal{Y}L)\left(\overrightarrow{F'}_{CL} + \overrightarrow{F'}_{CL}\right)$$

This corresponds to trapezoidal integration in the y-direction. The matching equation for the moment is

$$\overrightarrow{N} = (\mathcal{Y}CL - \mathcal{Y}L)[\overrightarrow{N'}_{CL} + \overrightarrow{N'}_{L} + (\vec{r}_{L} - \vec{r}_{CL}) \times \overrightarrow{F'}_{L}]$$

Where $\vec{r}_{L}$ is the position at which the forces are calculated. To demonstrate the capabilities of our reduced-order model, we used it to trim a hypersonic vehicle for steady-level Mach 8 flight at 26000 m altitude. The vehicle considered was the three-dimensional vehicle of Figures with the propulsive flow path geometries from. The propulsive model was found to have too much noise to complete this task easily, so a curve fit model was constructed. With the curve fit model constructed we were able to trim the vehicle for this state and visualize the performance of the propulsion system. It is shown that, the whole procedure of modeling of design hypersonic vehicles parts.

Trim Analysis: to demonstrate the capabilities of our reduced-order model, we used it to trim a hypersonic vehicle for steady-level. The vehicle considered was the three-dimensional vehicle of Figures with the propulsive flow path geometries from last figure. The propulsive model was found to have too much noise to complete this task easily, so a curve fit model was constructed. With the curve fit model constructed we were able to trim the vehicle for this state and visualize the performance of the propulsion system. We also present the state nearest to trim obtained using the full propulsive model.

e) Surrogate mode land propulsion system performance

The outcomes from the impetus model were profoundly delicate to little changes in approach and fuel-air identicalness proportion. Thus, we couldn't find a condition wherein all powers and minutes on the vehicle were adjusted utilizing a slope based minimization schedule. So as to make inclination based enhancement simpler, we created a proxy model by computing the propulsive execution on a consistently divided framework with 35 approaches and 35 fuel equality proportions all at a similar elevation and Mach number. The consequences of the propulsive model for every one of these conditions are appeared in Figure. The base and most extreme approaches considered were 0◦ and 4◦, separately. The base and maxi-mum fuel identicalness proportions considered were 0.5 and 3.0, individually. For conditions inside these restrictions of point of assault and comparability proportion yet not on the customary matrix, the presentation was determined utilizing cubic interjection. The outer streamlined model didn't utilize a substitute model. The extremely high identicalness proportions were considered on the grounds that the vast majority of the fuel doesn't consume in any event, when the proportionality proportion is underneath 1.0. In our propulsive model, the fuel is infused from only one wall, 10 which is the top divider in Fig. 7. In view of this uneven infusion and the way that the combustor is tall, the fuel can only with significant effort blend in with the oxygen close to the base of the combustor. Including more hydrogen past an identicalness proportion of 1.0 just builds dissemination. We found that a proportionality proportion of about 3.0 is expected to utilize the entirety of the oxygen in the combustor. This implies either including a portion of the fuel from the base mass of the combustor, expanding the fuel infusion weight, or utilizing a littler combustor would save fuel comparative with this plan.

ISSN No:-2456-2165

Model principle: A first-principle model of the 6-DOF dynamics of a generic hypersonic vehicle had developed by Ferneries where the 1D propulsion model has been borrowed from Ref. This Chapter focuses on development of a control design model and a control simulation model based on the FPM of Ref. The generic geometry of the vehicle considered in this work is shown in Figures 2.1 and 2.2, and the numerical values of the relevant geometric parameters are listed in Table 2.1. The available control surfaces (canard, elevator and rudder) are assumed to be Flat trapezoidal plates, with the left and right rudders inclined by an angle τr with respect to the normal vector on the upper body plane. The 6-DOF equations of motion of the vehicle in a body-fixed frame are given by Ref,

$$\dot{R} = \omega^{\times} R$$

$${}^{e}\dot{p} = Rv$$

$$\begin{pmatrix} m I_{3\times 3} & m r_g^{\times T} \\ m r_g^{\times} & J \end{pmatrix} \begin{pmatrix} \dot{\nu} \\ \dot{\omega} \end{pmatrix} = -\begin{pmatrix} m\omega^{\times}\nu + m\omega^{\times}\omega^{\times} r_g \\ \omega^{\times} J \omega \end{pmatrix} + \begin{pmatrix} \mathcal{F} \\ \mathcal{M} \end{pmatrix}$$

In the Equation, R ∈ SO(3) is the rotation matrix expressing the attitude of the vehicle with respect to an earth-fixed frame, ω = [p q r]T ∈ R3 is the angular velocity in body coordinates, ω× is the skew-symmetric matrix representing the cross product of vector ω (i.e. a×b = a×b for vectors a, b ∈R3), ep ∈R3 is the position of the center of gravity in inertial coordinates and ν = [u v w]T ∈R3 is the vehicle velocity in body frame. The vehicle mass, inertia matrix and location of the center of gravity are denoted respectively by m, J ∈ R3×3 and rg ∈ R3. Finally, F ∈ R3 and M ∈ R3 denote the vectors of external forces and moments, respectively. For the purpose of controlling the vehicle, the rotation and the oblations of the earthare ignored. In order to simplify the equations, a body-fixed coordinate frame was attached the center of mass of the vehicle.

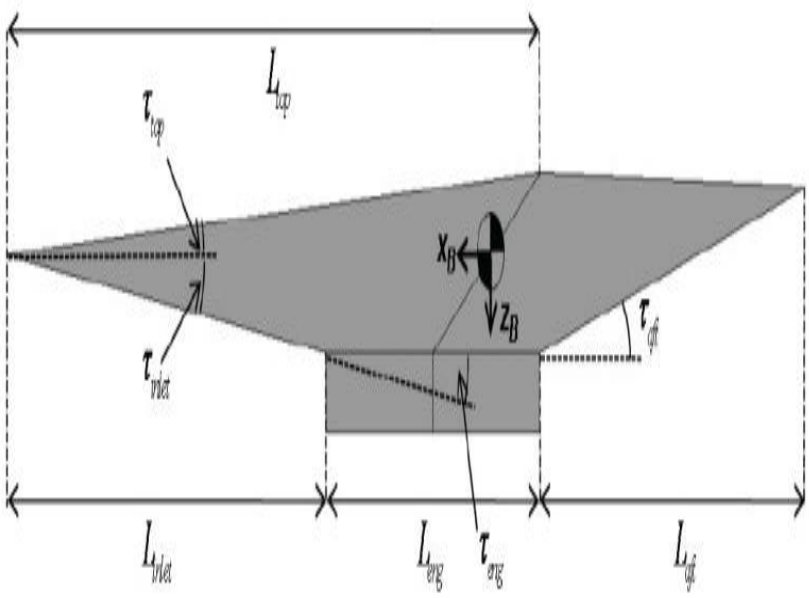

Fig. 12: Vehicle geometry in longitudinal plane.

Parameter	Description	Value
L_{inlet}	Inlet length	12 m
τ_{inlet}	Inlet turn angle	6 deg
L_{eng}	Engine/cowling length	8 m
τ_{eng}	Inlet to engine turn angle	6 deg
L_{aft}	Lower aftbody length	10 m
τ_{aft}	Engine to lower aftbody turn angle	15.82 deg
L_{top}	Upper forebody length	20 m
τ_{top}	Upper forebody turn angle	3 deg
τ_r	Rudder's incline angle	45 deg

Table 1: Fuselage geometric parameters

In this Chapter (not to be confused with the state variables of the controlled system as defined in Chapter 3), the vector x = (M∞, ¯q,α,β) collects the relevant functions of the state variables (R,p,ν,ω) given by Mach number, dynamic pressure, angle-of-attack and sideslip angle. The aircraft's Mach number is a dimensionless quantity defined as the ratio of airspeed and the local speed of sound [59]. Thespeed of sound depends on air pressure and density (or equivalently it depends on air temperature) where all these parameters depend on altitude.

The aircraft's angle of attack and sideslip angles are defined as follows;

$$\tan\alpha = \frac{w}{V_T} \quad , \quad \sin\beta = \frac{v}{V_T}$$

The forces and moments are comprised of the following terms

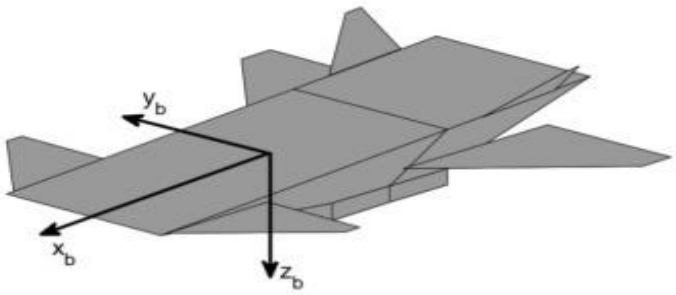

Fig. 13: 13 Aircraft's body frame

- The distributed aerodynamic forces and moments on the fuselage. Two-dimensional shock/expansion theory and the Taylor-McColl equations were used to derive the fuselage forces and moments.
- Aerodynamic forces on the control surfaces. These forces were derived using two-dimensional shock/expansion theory. Assuming the normal force on the control surfaces as single-point, their moments can be calculated using their forces and relative position of each control surface with respect to the center of mass of the aircraft
- Engine Thrust: The engine propulsion is calculated assuming that the airflow goes through isentropic diffuser first, and then a frictionless duct with heat addition as the combustor and finally the burned mixture goes through isentropic supersonic nozzle. The governing equations for all three stages of the propulsion can be found in Ref.
- The gravitational forces on the vehicle. Vehicle's mass is considered as a constant point mass located at the center of mass of the vehicle. Hence the gravitational force does not contribute to the aircraft's moments.

ISSN No:-2456-2165

CHAPTER 3

WINGED – CONEMODEL

A broadly utilized longitudinal model is the unbending body model in [7,11] for the winged-cone quickening agent configuration. In, the nonlinear longitudinal elements is created and numerical qualities for the streamlined coefficient are agent from. The winged-cone model is introduced as

$$\begin{aligned}
\dot{V} &= \frac{T\cos\alpha - D}{m} - \frac{\mu\sin\gamma}{r_E^2},\\
\dot{h} &= V\sin\gamma,\\
\dot{\gamma} &= \frac{L + T\sin\alpha}{mV} - \frac{(\mu - V^2 r_E)\cos\gamma}{Vr_E^2},\\
\dot{\alpha} &= q - \dot{\gamma},\\
\dot{q} &= \frac{M_{yy}}{I_{yy}}.
\end{aligned}$$

This model includes five state variables $X_h = [V, h, \alpha, \gamma, q]^T$ and control inputs $U_c = [\ \delta_{e,\ \Phi}\ ]^T$

The model related definitions of the HFV dynamics in [5] at Mach 15 and 110,000 feet are given as $\curlyvee_E$= h $+R_E$,$\bar{q} = \frac{1}{2}PV^2$, L = $\bar{q}SC_D$, T= $\bar{q}SC_{T,}M_{yy} = \bar{q}S_{\bar{c}}\ [C_M\ (\alpha) + C_M(\delta e)\ + C_M(q)$, C_L = 0.6203α, C_D = $0.6450\alpha^2$ + 0.0043378α + 0.003772, C_M (α) = − $0.035\alpha^2$ + 0.036617α + $5.3261 \times 10^{-6} C_M$ (q) = ($\bar{c}$/2V)q$(-6.796\alpha^2 + 0.3015\alpha - 0.2289)$.The control inputs related definition is as

$$\begin{cases} 0.02576\Phi, & if\Phi < 1,\\ 0.0224 + 0.00336\Phi, & otherwise; \end{cases}$$

Where$C_{x,x}$ = L ,D ,T ,M are the force and moment coefficient.

ISSN No:-2456-2165

CHAPTER 4

TRUTH AND CURVED FITTED MODEL

Reality model (TM) [13] was created by Blender and Doman [31] and Groves [32]. The model was inferred utilizing compressive flow hypothesis as an endeavor to broaden prior work done by Chavez and Schmidt [29]. A deduction dependent on Lagrange's conditions yields the conditions of movement of the longitudinal elements given by

$$\dot{V} = \frac{T\cos\alpha - D}{m} - g\sin\gamma,$$
$$\dot{h} = V\sin\gamma,$$
$$\dot{\gamma} = \frac{L + T\sin\alpha}{mV} - \frac{g\cos\gamma}{V},$$

$$\dot{\alpha} = q - \dot{\gamma},$$
$$\dot{q} = \frac{M_{yy}}{I_{yy}} + \frac{\tilde{\psi}_1\ddot{\eta}_1}{I_{yy}} + \frac{\tilde{\psi}_2\ddot{\eta}_2}{I_{yy}},$$
$$k_{1TM}\ddot{\eta}_1 = -2\zeta_1\omega_1\dot{\eta}_1 - \omega_1^2\eta_1 + N_1 - \tilde{\psi}_1\frac{M_{yy}}{I_{yy}} - \tilde{\psi}_1\tilde{\psi}_2\frac{\ddot{\eta}_1}{I_{yy}},$$
$$k_{2TM}\ddot{\eta}_2 = -2\zeta_2\omega_2\dot{\eta}_2 - \omega_2^2\eta_2 + N_2 - \tilde{\psi}_2\frac{M_{yy}}{I_{yy}} - \tilde{\psi}_1\tilde{\psi}_2\frac{\ddot{\eta}_2}{I_{yy}},$$

$$k_{1TM} = 1 + \frac{\tilde{\psi}_1}{I_{yy}},$$
$$k_{2TM} = 1 + \frac{\tilde{\psi}_2}{I_{yy}},$$
$$\tilde{\psi}_1 = \int_{-L_f}^{0} \hat{m}_f\varepsilon\phi_f(\varepsilon)\mathrm{d}\varepsilon,$$
$$\tilde{\psi}_2 = \int_{0}^{-L_a} \hat{m}_a\varepsilon\phi_a(\varepsilon)\mathrm{d}\varepsilon.$$

The bend fitted model (CFM) is a simplified, shut structure model that holds the basic qualities of the TM. The accompanying approximations are embraced in the investigation [13]: Here we can find out the value.

$$\begin{aligned}
T &\approx T_\Phi(\alpha)\Phi + T_0(\alpha)\\
&= [\beta_1(h,\bar{q})\Phi + \beta_2(h,\bar{q})]\alpha^3 + [\beta_3(h,\bar{q})\Phi + \beta_4(h,\bar{q})]\alpha^2 + [\beta_5(h,\bar{q})\Phi\\
&\quad + \beta_6(h,\bar{q})]\alpha + [\beta_7(h,\bar{q})\Phi + \beta_8(h,\bar{q})],\\
D &\approx \bar{q}S\left(C_D^{\alpha^2}\alpha^2 + C_D^{\alpha}\alpha + C_D^{\delta_e^2}\delta_e^2 + C_D^{\delta_e}\delta_e + C_D^0\right),\\
L &\approx L_0 + L_\alpha\alpha + L_{\delta_e}\delta_e = \bar{q}S\left(C_L^0 + C_L^{\alpha}\alpha + C_L^{\delta_e}\delta_e\right),\\
M_{yy} &\approx M_T + M_0(\alpha) + M_{\delta_e}\delta_e\\
&= z_T T + \bar{q}S\bar{c}\left(C_M^{\alpha^2}\alpha^2 + C_M^{\alpha}\alpha + C_M^0\right) + \bar{q}S\bar{c}C_M^{\delta_e}\delta_e,\\
N_1 &\approx N_1^{\alpha^2}\alpha^2 + N_1^{\alpha}\alpha + N_1^0,\\
N_2 &\approx N_2^{\alpha^2}\alpha^2 + N_2^{\alpha}\alpha + N_2^{\delta_e}\delta_e + N_2^0,\\
\bar{q} &= \frac{1}{2}\rho V^2,\\
\rho &= l\rho_0\exp\left[-\frac{h-h_0}{h_s}\right].
\end{aligned}$$

ISSN No:-2456-2165

In some studies, the weak couplings ˜ ψ1 and ˜ ψ2 between the rigid mode and flexible mode can be eliminated, then the flexible hypersonic flight model [30, 31] can be derived as

$$
\begin{aligned}
\dot{V} &= \frac{T\cos\alpha - D}{m} - g\sin\gamma, \\
\dot{h} &= V\sin\gamma, \\
\dot{\gamma} &= \frac{L + T\sin\alpha}{mV} - \frac{g\cos\gamma}{V}, \\
\dot{\alpha} &= q - \dot{\gamma}, \\
\dot{q} &= \frac{M_{yy}}{I_{yy}}, \\
\ddot{\eta}_i &= -2\zeta_i\omega_i\dot{\eta}_i - \omega_i^2\eta_i + N_i, i = 1, 2, 3.
\end{aligned}
$$

ISSN No:-2456-2165

CHAPTER 5

CURVED-FITTED MODEL AND CONTROL-ORIENTEDMODEL

The first guideline model (37) prompts conditions of movement in which the connections between control inputs and controlled yields are not unequivocal. For controller plan, a simplified model has been created following the methodology utilized in Ref. 16. The simplified model, alluded to as the bend fitted model (CFM), approximates the conduct of the accepted modes model by supplanting the streamlined and summed up powers and minutes with bend fitted approximations. The subsequent non-straight model offers the upside of being logically tractable (but still very perplexing) and increasingly appropriate for control structure, while holding the pertinent dynamical highlights of the first-rule model. The approximations of the powers and minutes utilized in the CFM are given as follows.

$$
\begin{aligned}
T &\approx C_{T,\Phi}(\alpha)\Phi + C_{A_d,\Phi}(\alpha)A_d + C_{T,0}(\alpha) + C_{T,\eta}\eta \\
M &\approx z_T T + \bar{q}\bar{c}SC_M(\alpha,\delta_e,\delta_c,\eta) \\
L &\approx \bar{q}SC_L(\alpha,\delta_e,\delta_c,\eta) \\
D &\approx \bar{q}SC_D(\alpha,\delta_e,\delta_c,\eta) \\
N_i &\approx N_i^{\alpha^2}\alpha^2 + N_i^{\alpha}\alpha + N_i^{\delta_e}\delta_e + N_i^{\delta_c}\delta_c + N_i^0 + N_i^{\eta}\eta
\end{aligned}
$$

Where the thrust-to-moment coupling coefficient zT and the mean aerodynamic chord $\bar{c}$ are given constants, $\bar{q}$ denotes dynamic pressure, and

$$
\begin{aligned}
C_{T,\Phi}(\alpha) &= C_T^{\Phi\alpha^3}\alpha^3 + C_T^{\Phi\alpha^2}\alpha^2 + C_T^{\Phi\alpha}\alpha + C_T^{\Phi} \\
C_{T,A_d}(\alpha) &= C_T^{A_d\alpha^3}\alpha^3 + C_T^{A_d\alpha^2}\alpha^2 + C_T^{A_d\alpha}\alpha + C_T^{A_d} \\
C_{T,0} &= C_T^{\alpha^3}\alpha^3 + C_T^{\alpha^2}\alpha^2 + C_T^{\alpha}\alpha + C_T^{0} \\
C_M(\alpha,\delta_e,\delta_c,\eta) &= C_M^{\alpha^2}\alpha^2 + C_M^{\alpha}\alpha + C_M^{\delta_e}\delta_e + C_M^{\delta_c}\delta_c + C_M^{0} + C_M^{\eta}\eta \\
C_L(\alpha,\delta_e,\delta_c,\eta) &= C_L^{\alpha}\alpha + C_L^{\delta_e}\delta_e + C_L^{\delta_c}\delta_c + C_L^{0} + C_L^{\eta}\eta \\
C_D(\alpha,\delta_e,\delta_c,\eta) &= C_D^{\alpha^2}\alpha^2 + C_D^{\alpha}\alpha + C_D^{\delta_e^2}\delta_e^2 + C_D^{\delta_e}\delta_e + C_D^{\delta_c^2}\delta_c^2 + C_D^{\delta_c}\delta_c + C_D^{0} + C_D^{\eta}\eta.
\end{aligned}
$$

In this study, the CFM is used primarily for simulation, while for the development of the controller a control-oriented model (COM) is employed, obtained from the CFM by neglecting the flexible dynamics. As a result, the flexible dynamics are not taken into account directly at the design level, but are considered as perturbations on the COM, and their effect evaluated in simulation. Consequently, the COM comprises of the five rigid-body state variables and four control inputs. Among the available control inputs, the canard surface defection (δc) will be used to decouple the lift force from the elevator, the fuel to air ratio (Φ) will be used to command thrust, and hence to control the vehicle velocity, while the elevator surface defection will ultimately be used to control the angular dynamics through the pitch moment. Since the diffuser area ratio (Ad) will not be used as independent control input, its value will be set to Ad = 1 for the remainder of the paper. Furthermore, to facilitate the development of the controller, the flight-path angle $\gamma = \theta - \alpha$ will be used in place of the pitch angle as a state variable. The equations of motions for the COM are given by

ISSN No:-2456-2165

$$
\begin{aligned}
\dot{V} &= \frac{T\cos\alpha - D}{m} - g\sin\gamma \\
\dot{h} &= V\sin\gamma \\
\dot{\gamma} &= \frac{L + T\sin\alpha}{mV} - \frac{g}{V}\cos\gamma \\
\dot{\alpha} &= -\frac{L + T\sin\alpha}{mV} + Q + \frac{g}{V}\cos\gamma \\
\dot{Q} &= \frac{M}{I_{yy}}
\end{aligned}
$$

$$
\begin{aligned}
T &\approx C_{T,\Phi}(\alpha)\Phi + \bar{C}_{T,0}(\alpha) \\
M &\approx z_T T + \bar{q}\bar{c}SC_M(\alpha, \delta_e, \delta_c, 0) \\
L &\approx \bar{q}SC_L(\alpha, \delta_e, \delta_c, 0) \\
D &\approx \bar{q}SC_D(\alpha, \delta_e, \delta_c, 0)
\end{aligned}
$$

$$
\bar{C}_{T,0} = \left(C_T^{A_d\alpha^3} + C_T^{\alpha^3}\right)\alpha^3 + \left(C_T^{A_d\alpha^2} + C_T^{\alpha^2}\right)\alpha^2 + \left(C_T^{A_d\alpha} + C_T^{\alpha}\right)\alpha + C_T^{A_d} + C_T^{0}.
$$

ISSN No:-2456-2165

CHAPTER 6

THE ANALYSIS OF DIFFERENT MODELS

A. *Comparison of deferent models*

Unlike winged-cone model, the TM incorporates the coupling between inflexible body increasing speeds and flexible body elements. Since the TM is mind boggling, CFM composes the articulation in shut structure. The statement of My in CFM contains the extra term zTT, where zT is a realized amount to represent the pitching second delivered by the under slung scramjet motor in the model [12]. As expressed in [13], the no minimum stage conduct results from the passing loss of lift that happens when the lift is activated to start a trip and the extra effector can be utilized to make up for the bothersome commitment of the lift to lift. The canard is set close to the nose of the airplane, forward of the focal point of gravity. The Cδe L thing is missing in the outflow of lift power for the COM on the grounds that the defection of the canard will be ganged with the lift defection utilizing a negative increase and the Cδe Lathing can be securely overlooked while Cδe M expands. The reemergence movement is made out of inward circle (precise rates) and external circle (crucial). The vector of control torque Mc is created by the streamlined surfaces, portrayed as $Mc = D0(\cdot)\delta$ where $D0(\cdot) \in R3\times6$ is affectability framework determined continuously based on table query information, $\delta \in R6$ is the vector of streamlined surface deflection. The strategic voyage and reemergence is deferent. For the journey stage, the longitudinal elements is considered with control objective to direct framework elevation and speed from a given arrangement of introductory qualities to wanted trim conditions with the following reference while the scramjet motor gives capacity to increasing speed. For the reemergence movement, the objective is to follow the predefined **precise which is administered by the streamlined** surface without scramjet motor so the vehicle could follow the ideal direction.

B. *Hypersonic flight control*

For hypersonic flight control, various plans have been proposed on straight controller, vigorous controller, versatile controller and clever controller. The emphasis is fundamentally on the best way to manage the framework uncertainty and ensure the steadiness of the shut circle framework. For instance, to manage the vulnerability, one can utilize the upper bound to develop the strong structure. Likewise thinking about that the vulnerability can be composed into directly parameterized structure; versatile control with parameter estimation could be contemplated. Moreover, the savvy control could be planned in the event that the vulnerability is the capacity of framework states. In this paper, for comprehensive investigation, the ongoing advancement in hypersonic flight control will be overviewed dependent on different route managing the elements rather than legitimately towards controller structure.

C. *Comparison of different control methods*

From the above investigation, the controller structure on the hypersonic flight model couldn't be straightforwardly built since the elements are perplexing. A few endeavors disentangling the structure are presented dependent on different beginning stages. For little irritation technique and info yield linearization, the straight model is gotten. For the T-S fluffy model, it gets the upside of fluffy framework and straight model while a trademark model is depicted continuously request differential condition. For little irritation technique, the direct model is estimated, even comparative with the model and the straight control hypothesis could be handily actualized on the linearized model. Since the direct model is on sure activity point, with enormous flight envelope, it requires gain planning around a few trim states of intrigue. The inconvenience is that it requires exact information on the model. Something else, the determined model can't speak to the highlights of the first elements. For the info yield linearization, the model is actually linearized utilizing input control signal. The relative degree ought to be determined and the nonlinearity turns out to be extremely mind boggling as request increments. At the point when the elements are known, input linearization could be cultivated and the dynamic reversal configuration could be applied. Nonetheless, vulnerability and aggravation exist and the specific model is inaccessible. Accordingly, extra vigorous

ISSN No:-2456-2165

structure and versatile thing ought to be remembered for the control to ensure framework soundness. For the "intermedium" model, the controller is actualized dependent on the great qualities professional vided by the "intermedium" model. For instance, the LMI based outcomes for the T-S fluffy model could be utilized. Likewise the trademark model speaks to the nonlinear elements with the second-request differential condition, in light of which the controller is anything but difficult to be developed. For the two techniques, "intermedium" model is approximated as the first elements however the deference between nonlinear elements and "intermedium" model is once in a while dissected. For instance, the exactness of T-S fluffy model is dependent on the guidelines. Anyway choosing the standards for nonlinear elements with predefined exactness is as yet an open issue. For the back-venturing plan, it doesn't change the elements into straight model and the controller could be planned bit by bit with powerful and versatile structure. With back-venturing structure, it is anything but difficult to consider different compels since the virtual control is produced for every condition. Somewhat, the structure is straightforwardly towards the nonlinear framework. A few endeavors are had a go at utilizing "indicator" without back-venturing [38,7] towards the asymptotic soundness of the shut circle framework. Since the "indicator" shows the direction of future yield under current control info and it doesn't present any data of framework states, it is difficult to incorporate the factor of states limitation. So for complex control reason there must be tradeoff between the control objective and the elements change.

ISSN No:-2456-2165

CHAPTER 7

FLIGHT DYNAMICS MODELRESULTS

The vehicle is trimmed for steady-level, Mach 8 flight at an altitude of 26 km, using the two available scramjet models. This task is achieved by determining a flight condition and set of control inputs that yield zero net force and moment on the vehicle. Trimming can be treated as a minimization problem, where the cost function is of the form;

$$J = \lfloor \bar{F} \bar{N}_B \rfloor [W] \begin{Bmatrix} \vec{F}_B \\ \vec{N}_B \end{Bmatrix}$$

Where W is a weighting matrix used to scale the various forces and moments. The cost function J is zero at the trimmed condition and strictly positive at all other conditions. The minimization is performed numerically in MATLAB R.
Using the function (constrained minimization) .The inertia properties of the vehicle used in the following trim analysis are given below.

Symbol	Name	Value
m	Mass	2.22×10^5 kg
I_{xx}	Moment of inertia about x-axis	3.42×10^6 kg $\cdot$ m^2
I_{yy}	Moment of inertia about y-axis	3.95×10^7 kg $\cdot$ m^2
I_{zz}	Moment of inertia about z-axis	3.95×10^7 kg $\cdot$ m^2
I_{xy}	Product of inertia	0 kg $\cdot$ m^2
I_{xz}	Product of inertia	0 kg $\cdot$ m^2
I_{yz}	Product of inertia	0 kg $\cdot$ m^2

Table 2: Vehicle inertia properties used for trim

The trimmed values for the flight dynamics states and control variables using the surrogate propulsion model are presented in Table 7.2. The trimmed values using the full propulsive model are presented in Table 7.3. Note that ψ, xE, and yE are ignored in this process because they do not contribute to the vehicle dynamics directly.

The trim state acquired utilizing the proxy model compares to a substantial consistent level flight condition, since all increasing speeds have an acceptably little size. Then again, the trim state got with the full propulsive model has a non-immaterial increasing speed in the x-bearing. In both trim cases, the lift deflection point is bigger than anticipated for a hypersonic vehicle. This is important to address the huge nose-down pitching second brought about by the remainder of the vehicle. Three potential solutions for this unfriendly second are moving the focal point of gravity, overhauling the nose of the vehicle, and actualizing control surfaces with more prominent position. The present nose of the vehicle needs more pressure on the bay incline and is gruff on the top. Turning around this will give more noteworthy pressure to the motor and create more lift close to the nose. The control surfaces on the vehicle are right now constrained to a couple of lifts.

ISSN No:-2456-2165

State	Name	Value
$\|\vec{v}_B\|$	Velocity magnitude	2.40 km/s
$-z_E$	Altitude	26 km
α	Angle of attack	2.89 deg
β	Sideslip angle	0 deg
θ	Pitch Euler angle	2.89 deg
ϕ	Roll Euler angle	0 deg
$\dot{v}_{B,x}$	x-component of $\dot{\vec{v}}_B$	-1.87×10^{-5} m/s^2
$\dot{v}_{B,z}$	z-component of $\dot{\vec{v}}_B$	1.45×10^{-5} m/s^2
$\dot{\omega}_{B,y}$	y-component of $\dot{\vec{\omega}}_B$	-1.52×10^{-8} rad/s^2
δ_e	Elevator deflection angle	26.9 deg
Φ	Scramjet fuel-air equivalence ratio	1.73

Table 3: Steady - Level Flight Trim Using Propulsion Surrogate

State	Name	Value
$\|\vec{v}_B\|$	Velocity magnitude	2.40 km/s
$-z_E$	Altitude	26 km
α	Angle of attack	2.86 deg
β	Sideslip angle	0 deg
θ	Pitch Euler angle	2.86 deg
ϕ	Roll Euler angle	0 deg
$\dot{v}_{B,x}$	x-component of $\dot{\vec{v}}_B$	4.28×10^{-1} m/s^2
$\dot{v}_{B,z}$	z-component of $\dot{\vec{v}}_B$	8.89×10^{-5} m/s^2
$\dot{\omega}_{B,y}$	y-component of $\dot{\vec{\omega}}_B$	-1.59×10^{-6} rad/s^2
δ_e	Elevator deflection angle	27.4 deg
Φ	Scramjet fuel-air equivalence ratio	1.95

Table 4: Steady-Level Flight Trim Using Full Propulsive Model

The area of the elevators or using all-moving elevons, the control surfaces will be able to provide the necessary forces at lower deflection angles. Shifting the vehicle's center of mass a couple of meters aft would also help to counter the nose-down moment. However, the other two design modification would still improve the vehicle's ability to maintain controlled flight for a range of conditions.

ISSN No:-2456-2165

CHAPTER 8

CONCLUSION ANDPOTENTIAL FUTURERESEARCH

A. Conclusion

A decreased request model was created to perform inflexible body flight elements examination on a hypersonic vehicle. The model can be utilized on a wide class of scramjet vehicles that are evenly symmetric and have roughly two-dimensional channels and spouts. The model doesn't think about the impacts of a flexible vehicle, yet it gives investigation to each significant segment of the vehicle. For every part, the models are proposed to incorporate, in any event subjectively, the entirety of the nonlinear conduct of a genuine hypersonic vehicle, including stun associations, flameout, and so forth. The main flight elements investigation acted in the current conversation was cutting the vehicle for consistent level flight. The drive model was found to have ridiculous affectability, and a bend fit model was built dependent on the aftereffects of the impetus model. Various proposals for upgrades in vehicle configuration were found because of the trim examination. For example a higher pressure proportion in the gulf would both increment push and surrender a higher nose second. Without certain changes to the structure, cutting the vehicle at a chose flight condition required producing additional drag with the flaps to neutralize the nose-down second and cutting at higher Mach numbers demonstrated unimaginable. In spite of the fact that activity over a wide envelope of flight conditions is trying for any aviation vehicle, this is especially valid for hypersonic vehicles for which pretty much every property is nonlinear. What's more, this structure has been stretched out for future models that will incorporate aerothermoelastic impacts necessary for a total examination of a hypersonic vehicle. This structure can likewise be applied as a device in control configuration, control assessment, and direction examination.

B. POTENTIAL FUTURE RESEARCH

From the previously mentioned study, we see that both direct and nonlinear strategies have been seriously concentrated on hypersonic flight control. Be that as it may, current controller is proposed by the structure of HFV elements. Somewhat, the thought is practically near the ordinary airplane control. This is the fundamental issue lying in current hypersonic control applications and more specific qualities of hyper-sonic flight elements ought to be contemplated for controller plan. So there are key and fundamental issues that merit examining further. Taking into account the capacity for the controller, it ought to be vigorous to obscure condition and adjust quickly with framework change. Likewise for the issue lying in hypersonic flight with huge flight envelope, actuator immersion, aerothermoelastic effect and elements association should draw more consideration. For X-30 or X-43A, the primary lift to generate surface is the body itself due to inefficiency of using a thin wing. So during the flight, requirement of large lift force may result in unaffordable elevator deflection. Also the sudden environmental disturbance may cause the instantaneous saturation of the elevator deflection and it will deteriorate the performance or even make the system unstable. Dead-zone input nonlinearity is a non-differential function that characterizes certain non-sensitivity for small control inputs. The presence of such nonlinearity in feedback control systems may cause severe deterioration of the system performances. HFV is one kind of unmanned aircraft and the controller is implemented by digital computer. It is important to analyze how the system uncertainty would effect the control performance since the error could be cumulated with the system order. The derivation of discrete controller with back-stepping design may result in the requirement of a really large control input. This is not reasonable for real application and it is crucial for the controller to be equipped with the capability of “looking ahead and prediction”. Though the controllers have been proved to make the system stable, sometimes the control input is subjected to high frequency oscillation. In real life the oscillation may lead to instability of the vehicle and thus the controllers cannot be employed. From the above analysis, to make the flight control efficient, the actuator dynamics should be taken into consideration to improve safety, reliability, maintainability of the flight task for hypersonic vehicle.

ISSN No:-2456-2165

Dynamics interactions and transient performance: The streamlined effect of the versatile airframe, impetus framework, and basic elements are exceptionally intuitive and the related qualities stay questionable and difficult to anticipate because of absence of sufficient tests and deficiency of ground test offices [1]. The flexible states show up in the elements and are combined with the pitch rate. As of now the controllers either overlook the flexible states or think about it as aggravation. In spite of the fact that reenactments show the practicality under certain condition, more head examination ought to be paid on the decoupling of different time-scale states. Additionally flexible difference in the shape changes conditions for working of scramjet motor. Besides, the annoyance of impetus framework in a roundabout way impacts the longitudinal elements, the versatile mode varieties. So the versatile airframe, impetus framework, and auxiliary elements communicate on one another emphatically. In any case, for controller plan, the factor of coupling between impetus framework and vehicle body was not "truly" investigated. It is realized that the elements are temperamental, profoundly coupled and affected by significant model uncertainty. The hypersonic vehicles fly at such rapid and little information on the streamlined features exists. In this way on the off chance that the transient execution is terrible, at that point the framework may go precarious. So further the research should target investigating the transient execution to guarantee the safe and efficient running of framework.

ISSN No:-2456-2165

ACKNOWLEDEMENTS

- When I first entered the engineering field in the fall of 2017 to pursue a Bachelor's degree in Aeronautical Engineering, I never would have that I would present a Bachelor's thesis at NANCHANG HANKONG UNIVERSITY. After becoming fascinated with aerospace during junior design projects, the past four years have been filled with spectacular opportunities to learn and become engaged with the aviation field.
- Foremost, I would like to express my sincere gratitude to my advisor Associate Professor Longsheng Chen for extending the opportunity to study Aerospace Engineering related knowledge. I also extend my thanks to Mr. Zhang and all staff of the International School of Nanchang Hangkong University for their Constant Support throughout my undergraduate courses.
- His guidance and support about the thesis has led to growth in knowledge and skill as well as development as an individual. The numerous research areas and networking opportunities fostered curiosity in the realm of hypersonic which have ultimately led to this thesis. I would also like to thank say my brother for help me to complete of my thesis. Their technical support, enthusiasm about hypersonic and encouragement helped immensely throughout the thesis process.

I would like to thank my family for their unconditional love and support throughout these 4 years of graduate school. Finally, I would like to thank teachers and friends that I have met during my time at Nanchang Hangkong University. Thank you all for accompanying me along this journey.

REFERENCES

[1.] Abzug, M., and Larrabee, E., *Airplane Stability and Control: A History of the Technologies that Made Aviation Possible*, Cambridge University Press, 2002.
[2.] Abzug, M., *Computational Flight Dynamics*, AIAA Press, 1998.
[3.] Anderson, J., *Fundamentals of Aerodynamics*, McGraw-Hill, 2011.
[4.] Anderson, J., *Aircraft Performance and Design*, McGraw-Hill, 1999.
[5.] Anderson, J., *A History of Aerodynamics*, Cambridge University Press, 1997.
[6.] Ashley, H., *Engineering Analysis of Flight Vehicles*, Addison-Wesley, 1974.
[7.] Asselin, M., *An Introduction to Aircraft Performance*, AIAA Press, 1997.
[8.] Babister, A., *Aircraft Dynamic Stability and Response*, Pergamon Press, 1980.
[9.] Beard, R., and McLain, T., , , *Small Unmanned Aircraft* Princeton University Press, 2012.
[10.] Blakelock, J., *Automatic Control of Aircraft and Missiles*, J. Wiley & Sons, 1991.
[11.] Cook, M., *Flight Dynamics Principles*, Elsevier, 2007.
[12.] Etkin, B., and Reid, L., *Dynamics of Atmospheric Flight*, J. Wiley & Sons, 1972.
[13.] Gibson, J., *The Definition, Understanding and Design of Aircraft Handling Qualities*, Delft University Press, 1997 .
[14.] H odgkinson, *Aircraft Handling Qualities*, AIAA Press, 1999.
[15.] Howard, F., and Gunston, B., *The Conquest of the Air*, Random House, 1972.
[16.] Mair, W., and Birdsall, D., *Aircraft Performance*, Cambridge University Press, 1992.
[17.] Klein, V. and Morelli, E.A., *Aircraft System Identification - Theory and Practice*, AIAA Education Series, 2006.
[18.] Davis,Asymptotic analysis of hypersonic boundary layers over an adiabatic wall with deformations,2009
[19.] Lowry, J., *Performance of Light Aircraft*, AIAA Education Series, 1999.
[20.] Chaofang Hu,Polytopic linear parameter varying model-based tube model predictive control for hypersonic vehicles 2007
[21.] McClamroch, N. H., Steady Aircraft Flight and Performance, Princeton University Press, 2011.
[22.] McCormick, B., Aerodynamics, Aeronautics, and Flight Mechanics, J. Wiley & Sons, 1994.
[23.] McRuer, D., Ashkenas, I., and Graham, D, *Aircraft Dynamics and Automatic Control*, Princeton University Press, 1973.
[24.] Miele, A., *Flight Mechanics: Theory of Flight Paths*, Addison-Wesley, 1962.
[25.] Napolitano, M., *Aircraft Dynamics: From Modeling to Simulation*, J. Wiley & Sons, 2011.
[26.] Nelson, R., *Flight Stability and Automatic Control*, McGraw Hill, 1998.
[27.] XU Bin,*An overview on flight dynamics and control approaches for hypersonic vehicles, 2015.*
[28.] Yuri Ivanovich Khlopkov, Sergey Leonidovich Chernyshev, Modern Trends in the Development of Reusable Aerospace System ,2014)
[29.] Nicolai, L., *Fundamentals of Aircraft Design*, School of Engineering, University of Dayton, 1975.
[30.] Ojha, S., *Flight Performance of Aircraft*, AIAA Press, 1995.
[31.] Pamadi, B., *Performance, Stability, Dynamics, and Control of Airplanes*, AIAA Press, 2004. 1975.
[32.] Ojha, S., *Flight Performance of Aircraft*, AIAA Press, 1995.
[33.] Mohammad Shakiba-Herfeh, Modeling and Nonlinear Control of a 6-DOF Hypersonic Vehicle, 2015
[34.] Perkins, C., and Hage, R., *Airplane Performance Stability and Control*, J. Wiley & Sons, 1949.
[35.] Phillips, W. F., *Mechanics of Flight*, J. Wiley & Sons, 2004.
[36.] Pratt, R. W., ed, *Flight Control Systems*, AIAA Press, 2000.
[37.] Raymer, D., *Aircraft Design: A Conceptual Approach*, AIAA Press, 1989.
[38.] Rolfe, J., and Staples, K., *Flight Simulation*, Cambridge University Press, 1986.
[39.] Schlichting, H., and Truckenbrodt, E., *Aerodynamics of the Airplane*, McGraw-Hill Book Co., 1979.
[40.] Derek J. Dalle. Hypersonic Vehicle Flight Dynamics with Coupled Aerodynamics and Reduced-order Propulsive Models, 2010

[41.] Michael A. Bolender‡ David B. Doman ,Nonlinear Robust/Adaptive Controller Design for an Air-breathing Hypersonic Vehicle Model 2007